A first isothermal approach to 3D sloshing for aircraft hydrogen tanks.

Ignacio Sánchez-Ojeda
Javier Calderon-Sanchez
Leo M. González
ETSI Navales, CEHINAV,
Universidad Politécnica de Madrid, UPM
Madrid, SPAIN

I. Introduction

The aerospace industry is currently facing important challenges and probably one of the most important ones is the obtention of an effective decarbonization using clean fuels. In this context, the use of hydrogen as a clean fuel is one of the solutions that the industry is currently evaluating. The HASTA EU project [1] (*Hydrogen Aircraft Sloshing Tank Advancement*) aims to investigate the storage of Liquid Hydrogen (LH2) for airborne use as fuel in large civil aircraft. One of the most important parts of this disruptive change is the design of the fuel tank, where the two-phase liquid-vapour hydrogen is stored before being pumped into the engines. The typical inertial forces due to the different accelerations of the aircraft give rise to the phenomenon of sloshing, which implies complex heat and mass transfer processes. The characterization of the different sloshing regimes is a crucial part, as this phenomenon affects the control of the thermodynamic variables inside the tank, which has important consequences on the injection of fuel into the engine. This work presents an initial approach to the sloshing problem when a realistic horizontal cylindrical tank geometry is used keeping in mind the objective of determining the different sloshing regimes.

The numerical method selected to study this problem is SPH as it is well known its good performance for free surface flows. The roadmap is first having a good validation of the SPH method for the isothermal case, and secondly, the non-isothermal case will be studied adding the heat transfer and phase change to the problem.

Our work focuses mainly on developing methods for simulating three-dimensional problems. Some previous work on 3D problems has been done, such as [2] and [3]. In [2], Sun et al. discuss the inclusion of a particle shifting technique (PST) in weakly compressible SPH models. They tested their approach in a 3D model of a tank with straight walls. Pilloton et al. study in [3] the viscosity effects in the swirling of different fluids in a cubic tank. Both studies, as they have straight walls, present an easier discretization of the initial fluid domain. For the horizontal cylindrical tank used in the HASTA project, a new approach has been developed. In this, the boundaries are discretized through the *Boundary Integrals method*, such as in [4]. For the fluid domain, a Cartesian distribution of possible particles is generated, and suitable particles are discerned using *signed distance functions* (SDF) using the analytical definition of the boundaries. With this approach, a fairly good approximation of the initial fluid domain can be done, independently of the boundaries of the domain, as long as these are a good representation of the analytical definition of the boundaries.

For validating the results, the SPH simulations will be compared to previous studies. The model presented in [5] will be used for qualitative validation, as the sloshing modes and general behaviour that appear in the SPH simulations are compared with the ones characterized by Grotle and Æsøy. The moments that the sloshing produces on the tank will be also calculated. The results of the SPH simulations will be compared against the ones presented in [5].

II. Equations

For this problem, the formulation presented in [6] is used. The Navier-Stokes equations for a weakly-compressible and barotropic fluid can be written in Lagrangian form as in the system of equations 1 where $\frac{D}{Dt}$ represents the Lagrangian derivative, p is the pressure field, $\mathbf{g}$ is the generic external volumetric force field, and $\mathbf{V}$ the viscous stress tensor. The material derivative of a fluid particle position $\mathbf{r}$ defines the flow velocity.

$$\begin{cases} \dfrac{D\rho}{Dt} = -\rho\nabla\cdot\mathbf{u}, \quad p = f(\rho), \\ \dfrac{D\mathbf{u}}{Dt} = \dfrac{1}{\rho}\nabla p + \dfrac{1}{\rho}\nabla\cdot\mathbf{V} + \mathbf{g} + \mathbf{\Omega}_{ST}, \\ \dfrac{D\mathbf{r}}{Dt} = \mathbf{u}, \end{cases} \tag{1}$$

As a weakly compressible formulation is assumed, pressure is determined as a function of density fluctuations through a linearized equation of state (EOS) such as $p = c_0^2(\rho - \rho_0)$, in which c_0 is the sound speed, defined as 10 times the maximum expected velocity of the fluid.

The viscous stress tensor can be rewritten in the form of

$$\mathbf{V} = \lambda\,\mathrm{tr}(\mathbf{D})\mathbf{I} + 2\mu\mathbf{D}, \tag{2}$$

where $\mathbf{D}$ is the strain rate tensor $\mathbf{D} = (\nabla u + \nabla u^T)/2$, $\mathbf{I}$ the identity tensor, and λ and μ the bulk and dynamic coefficients, respectively.

The δ-SPH formulation proposed by Antuono et al. in [7] is used. The discrete set of particles in SPH is governed then by the system of equations:

$$\begin{aligned}
\frac{D\rho_i}{Dt} &= -\rho_i \sum_j (\mathbf{u}_j - \mathbf{u}_i) \cdot \nabla W_{ij} V_j + h c_s \delta \sum_j \mathcal{D}_{ij} \cdot \nabla W_{ij} V_j, \\
\frac{D\mathbf{u}_i}{Dt} &= \mathbf{g} - \frac{1}{\rho_i} \sum_j (p_i + p_j) \nabla W_{ij} V_j \\
&\quad + \frac{\mu K}{\rho_i} \sum_j \Pi_{ij} \nabla_i W_{ij} V_j + \mathbf{\Omega}_{ST}, \\
\frac{D\mathbf{r}_i}{Dt} &= \mathbf{u}_i + \delta \mathbf{u}_i, \quad p = p_0 + c_s^2(\rho_i - \rho_0),
\end{aligned} \tag{3}$$

where j are the indexes of the neighbour particles, V_j is the volume of the neighbour particle j and $W_{ij} = W(\mathbf{r_j} - \mathbf{r_i}, h)$ is the kernel function at constant smoothing lenght h. $\nabla_i W_{ij}$ is the derivative of the kernel function with respect to the ith particle. The Wendland C2 kernel is being used, with a h/dr ratio equal to 2. The added diffusive terms $\mathcal{D}_{ij}$ and Π_{ij} are the ones presented in [7].

A *Particle Shifting Technique* (PST) like the one presented in [2] is used to avoid tensile instability. The shifting velocity $\delta\tilde{u}_i$ is introduced as

$$\delta\tilde{u}_i = -U_{\text{ref}}\, 2h \sum_j \left[1 + 0.2 \left(\frac{W_{ij}}{W(\text{dr})}\right)^4\right] \nabla_i W_{ij} V_j. \tag{4}$$

As only one phase is considered in this work, a free-surface tracking algorithm must be implemented to avoid shifting velocities normal to the free surface. The free surface algorithm implemented in [8], where the eigenvalues λ_i of the renormalization matrix L^{-1} and the normals $\mathbf{n_i}$ are used.

$$\mathbf{n}_i = \frac{\langle\nabla\lambda\rangle_i}{\|\langle\nabla\lambda\rangle_i\|}, \ \langle\nabla\lambda\rangle_i = -\sum_j (\lambda_j - \lambda_i) L_i \nabla_i W_{ij} V_j. \tag{5}$$

$$L_i := \left(\sum_j \mathbf{r}_{ji} \otimes \nabla_i W_{ij} V_j\right)^{-1}. \tag{6}$$

Once the free-surface is characterized, the shifting velocity δu_i is calculated from $\delta\tilde{u}_i$ as in [2].

As discussed in [6], a general surface tension field $\mathbf{\Omega}_{ST}$ is added to the momentum equation to deal with interface surface forces:

$$\mathbf{\Omega}_{ST} = -\frac{\sigma}{\rho_i} \sum_j (\mathbf{n}_j - \mathbf{n}_i) \cdot \nabla W_{ij} V_j \mathbf{n}_i, \tag{7}$$

For the treatment of the solid boundary, the boundary integrals approach described by Cercos-Pita in [4] is used. In the boundary integrals formulation, the differential operators are defined in the presence of a boundary as

$$\langle\nabla f\rangle_i = \frac{1}{\gamma_i} \left(\sum_{j_*} f_{j_*} \cdot \nabla W_{ij} V_{j_*} + \sum_j f_j \cdot \mathbf{n}_j W_{ij} s_j\right), \tag{8}$$

where f_i is a generic field function, $\mathbf{n}$ the normal of the surface, pointing outwards, s_j the area of the surface element and γ_i the Shepard renormalization factor, that is computed geometrically trough the semi-analytical approach discussed in [9]

III. Results

The geometry used is that presented by Grotle and Æsøy in [5], with a length of $L = 0.89$ m and diameter $D = 0.35$ m. The geometry of the cylinder has been meshed using a commercial code. The cells have then been decomposed into centroids, areas, normal, and tangents, which are the input data for generating the boundary integral elements. The SPH solver used is AQUAgpusph [10].

For generating the possible particles for the initial fluid state, a cartesian mesh of particles is created using as limits the length and diameter of the cylinder, and placing the starting particle at a distance of 0.5 times dr, being dr the initial spacing between particles. Once the possible particles are created, the final particles are selected using SDF functions. As criteria, is established that a particle is suitable if its signed distance values to the analytical expressions of the walls are lower than $-0.5\,dr$. This method allows to place the particles as close as possible to the initial state, reducing the time for an initial settlement of the particles. Also, the method makes it possible to use more complex geometries than the usual prism or orthogonal shapes used in the literature. The particle distribution can be observed in Figure 1. The discretization of the boundary affects the generated fluid volume, and further improvements are being researched, to ensure the expected fluid volume.

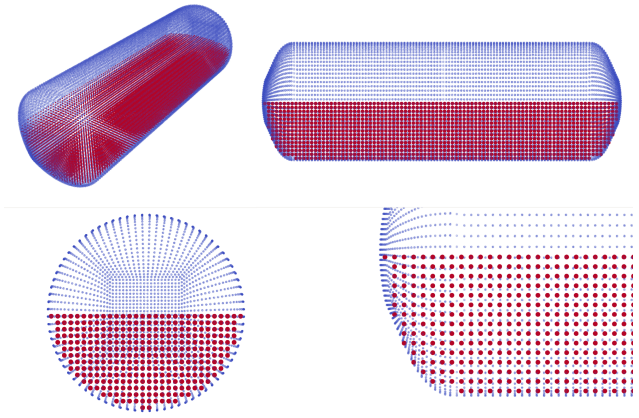

Fig. 1. Particle Distribution. Resolution of 15 particles in the vertical direction at the center plane of the cylinder.

Some results have been obtained for the same frequencies selected by Grotle and Æsøy in [5] ($f = 0.29,\ 0.40$ and 0.57

Hz). The tank oscillates around its transversal axis (Y-Axis in Figure 2). The rotation of the tank is defined by the law $\theta = A\sin(\omega t)$, where A is the amplitude, which in this case is 3 degrees, and ω which is $2\pi f$. The motion law of the tank also includes 5 seconds at the beginning with the tank static, to help the initialization of the fluid particles, and then the oscillation starts with a ramp function modification in the amplitude term (for 2 periods). Then the tank oscillates for 20 periods. The simulations have been done in a NVIDIA A100 graphic card. A coarse resolution of 15 particles in the vertical direction was established, resulting in 28074 fluid particles and 12000 boundary elements. Grotle and Æsøy characterise 3 different regimes at these frequencies: Small deformations, oscillating waves and jet formation. These have been satisfactorily identified in the AQUAgpusph simulations. In Figure 2 the jets that show up at the ends of the tank at the highest test frequency can be seen. The detected free surface is represented in red. The surface detection algorithm implemented is the one presented by Marrone et al. in [8]. Further improvements such as turbulence models and finer resolutions will be used.

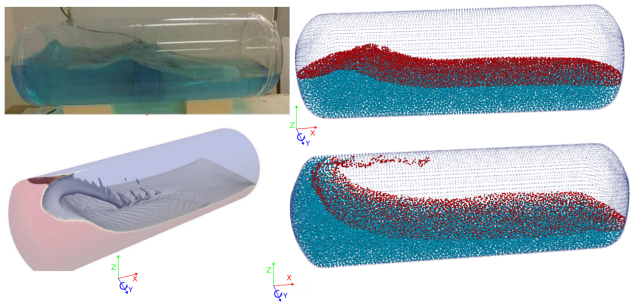

Fig. 2. Jets formed in study case 3 ($f = 0.57$ Hz). Rotation around the Y-Axis in the image. Left: Grotle and Æsøy [5]. Right: Snapshot from AQUAgpusph. Detected free surface in red.

The study of the forces and moments suffered by the tank are also of interest, to identify the different sloshing regimes and the events that trigger the changes from one mode into another. In Figures 3 and 4 the non-dimensional moments measured for $f = 0.40$ and 0.57 Hz are shown. Moments are non-dimensionalized with the diameter of the tank and a mean $f = 0.5$ Hz. Moments signal is filtered with a Low Pass Fourier Filter for a cut-off frequency of 15 Hz to reduce noise. As expected, the moment grows as the frequency gets closer to the resonance point.

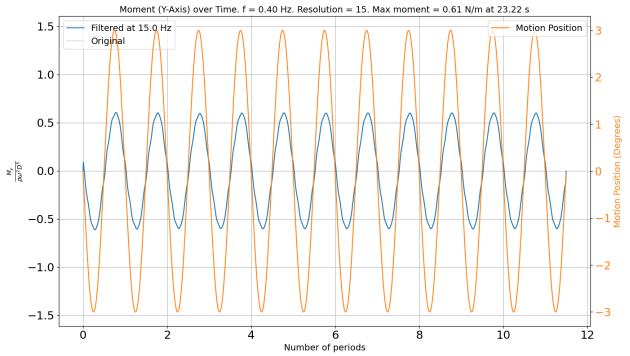

Fig. 3. Moments in the roll axis. $f = 0.40$ Hz. Motion of the tank in orange.

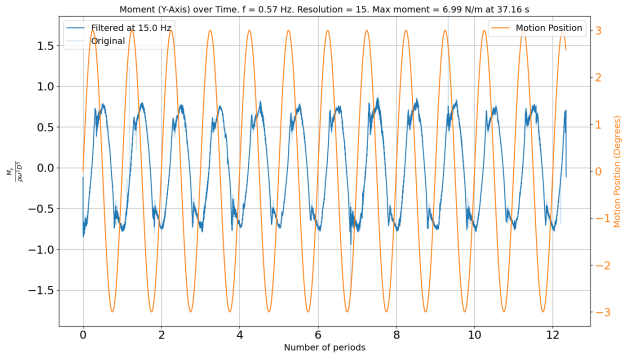

Fig. 4. Moments in the roll axis. $f = 0.57$ Hz. Motion of the tank in orange.

Acknowledgment

Funded by the European Union (**HASTA, 101138003**). Views and opinions expressed are, however, those of the author(s) only and do not necessarily reflect those of the European Union. Neither the European Union nor the granting authority can be held responsible for them.

References

[1] HASTA. (2024) Hydrogen aircraft sloshing tank advancement. [Online]. Available: https://hasta-project.eu/

[2] P. Sun, A. Colagrossi, S. Marrone, M. Antuono, and A.-M. Zhang, "A consistent approach to particle shifting in the -plus-sph model," *Computer Methods in Applied Mechanics and Engineering*, vol. 348, pp. 912–934, 2019. [Online]. Available: https://www.sciencedirect.com/science/article/pii/S0045782519300702

[3] C. Pilloton, J. Michel, A. Colagrossi, and S. Marrone, "A numerical investigation on three-dimensional swirling instability in viscous sloshing flows," *Applied Ocean Research*, vol. 138, p. 103621, 09 2023.

[4] J. Cercos-Pita, "Aquagpusph, a new free 3d sph solver accelerated with opencl," *Computer Physics Communications*, vol. 192, pp. 295–312, 2015. [Online]. Available: https://www.sciencedirect.com/science/article/pii/S0010465515000909

[5] E. L. Grotle and V. Æsøy, "Numerical simulations of sloshing and the thermodynamic response due to mixing," *Energies*, vol. 10, no. 9, 2017. [Online]. Available: https://www.mdpi.com/1996-1073/10/9/1338

[6] C. S. Javier, M. C. Jon, and G. L. Miguel, "Computational scaling of sph simulations for violent sloshing problems in aircraft fuel tanks," *Acta Mechanica Sinica*, vol. 39, p. 722051, 2023. [Online]. Available: https://doi.org/10.1007/s10409-022-22051-x

[7] M. Antuono, A. Colagrossi, and S. Marrone, "Numerical diffusive terms in weakly-compressible sph schemes," *Computer Physics Communications*, vol. 183, no. 12, pp. 2570–2580, 2012. [Online]. Available: https://www.sciencedirect.com/science/article/pii/S0010465512002342

[8] S. Marrone, A. Colagrossi, D. Le Touzé, and G. Graziani, "Fast free-surface detection and level-set function definition in sph solvers," *Journal of Computational Physics*, vol. 229, no. 10, pp. 3652–3663, 2010. [Online]. Available: https://www.sciencedirect.com/science/article/pii/S0021999110000343

[9] J. Calderon-Sanchez, J. Cercos-Pita, and D. Duque, "A geometric formulation of the shepard renormalization factor," *Computers Fluids*, vol. 183, pp. 16–27, 2019. [Online]. Available: https://www.sciencedirect.com/science/article/pii/S0045793019300416

[10] J. L. Cercos Pita, A. Souto Iglesias, and L. M. Gonzalez, "AQUAgpusph: Another QUAlity GPU-SPH," http://canal.etsin.upm.es/aquagpusph/, 2013, accessed: 2025-01-19.